The next Zika virus outbreak will affect young women of reproductive age disproportionately: mathematical modeling study

Michel J. Counotte[1,2], Christian L. Althaus[1], Nicola Low[1], and Julien Riou[1]

[1]Institute of Social and Preventive Medicine, University of Bern, Bern, Switzerland
[2]Graduate School for Cellular and Biomedical Sciences, University of Bern, Bern, Switzerland

June 6, 2019

Abstract

Zika virus (ZIKV) is a mosquito-borne flavivirus. In 2016, Managua, the capital city of Nicaragua experienced a Zika virus outbreak. Amongst confirmed cases, seropositivity increased with age and >50% of the adult population had ZIKV antibodies. The duration of immunity to ZIKV remains unclear. We used an agent-based model in a Bayesian framework to describe the dynamics of immunity to ZIKV, and predict the future age-specific risk of ZIKV infection in the population of Managua. We also investigated the potential impact of a ZIKV vaccine under different assumptions about the persistence of immunity. Assuming lifelong immunity, the risk of a ZIKV outbreak will remain low until 2035 and rise above 50% in 2047. Young women of reproductive age will be at highest risk of infection during the next ZIKV outbreak. ZIKV vaccine development and licensure are urgent, to attain the maximum benefit in reducing the population-level risk of infection and the risk of adverse congenital outcomes.

1 Introduction

Zika virus (ZIKV) is a flavivirus, which is transmitted primarily by mosquitoes of the genus *Aedes*. Before 2007, circulation of the virus only occurred sporadically in African and Asian countries (Wikan and Smith, 2016; Kohl and Gatherer, 2015). Between 2007 and 2013, ZIKV caused large-scale epidemics of infection, characterized by rash and fever, in Micronesia (Duffy et al., 2009), French Polynesia (Cao-Lormeau et al., 2014) and other Pacific islands (Wikan and Smith, 2016). ZIKV virus probably became established in *Aedes aegypti* mosquitoes in the Americas between 2013-2014, (Faria et al., 2016; Zhang et al., 2017) and then spread rapidly across the continent. In 2015, doctors in Brazil started reporting clusters of infants born with microcephaly and of adults with Guillain-Barré syndrome, a paralyzing neurological condition, resulting in the declaration by the World Health Organization (WHO) of a Public Health Emergency of International Concern (PHEIC) (World Health Organization, 2016). WHO stated, in September 2016, that ZIKV in pregnancy was the cause of the clusters of microcephaly, and other adverse congenital outcomes (Krauer et al., 2017; Counotte et al., 2018). The risk of an affected pregnancy appears highest during first trimester, with estimates between 1.0 and 4.5% (Cauchemez et al., 2016; Johansson et al., 2016). By the beginning of 2018, over 220,000 confirmed cases of ZIKV infection had been reported from Latin America and the Caribbean (PAHO, 2019), which is estimated to be only 1.02% (± 0.93%) of the total number of cases, based on mathematical modelling studies (Zhang et al., 2017).

Protective immunity conferred by infection, combined with high attack rates and herd immunity, can explain the ending of arbovirus epidemics and the lack of early recurrence (Dietz, 1975), as has been seen with ZIKV. The duration of protective immunity induced by ZIKV infections remains uncertain, since immunity to ZIKV infection was not studied extensively, until the 2014-16 outbreaks. Evidence from seroprevalence studies in French Polynesia and Fiji found that ZIKV neutralizing antibodies levels decrease with time (Henderson et al., 2019). If the fall in antibody levels means that people are susceptible to infection again, population level ZIKV immunity might be declining already. Even if protective immunity is lifelong, the risk of a new ZIKV outbreak will rise as susceptible newborns replace older individuals, lowering the overall proportion of the population that is immune. A modelling study, based on data from the 2013 epidemic in French Polynesia, estimated that ZIKV outbreaks are unlikely to occur for 12 to 20 years, assuming lifelong immunity (Kucharski et al., 2016).

A direct consequence of population renewal will be an unequal distribution of immunity by age group, with younger age groups at higher risk from a new epidemic than older people (Ferguson et al., 2016). That effect will be amplified if ZIKV attack rates are lower in children than adults. Assessing the risk of ZIKV infection in women of reproductive age is essential because ZIKV infection in pregnancy, leading to adverse congenital outcomes, has such important implications for individuals, for public health and for investment in surveillance and mitigation strategies, including vector control, early warning systems, and vaccines (Abbink et al., 2018; World Health Organization, 2018).

Researchers in Managua, Nicaragua were the first to report the seroprevalence of ZIKV antibodies in population-based surveys, according to age (Zambrana et al., 2018). The first cases of autochthonous ZIKV infection in Nicaragua were reported in January, 2016, and an epidemic was observed between July and December of that year. Through case-based surveillance, the public health authorities of Nicaragua reported a total of 2,795 people with ZIKV detected by reverse transcriptase (RT) PCR over this period (PAHO, 2019). The number of symptomatic infections is likely much higher, owing to under-reporting. Furthermore, ZIKV infection is asymptomatic in 33 to 87% of cases (Haby et al., 2018), and is generally not identified by surveillance systems. Shortly after the end of the 2016 epidemic, Zambrana et al. analyzed sera from two large population-based surveys in Managua to measure the prevalence of IgG antibodies against ZIKV in 2- to 14-year olds (N=3,740) and 2- to 80-year olds (N=2,147) (Zambrana et al., 2018). The authors reported ZIKV seroprevalence of 36.1% (95% confidence interval, CI 34.5, 37.8%) among the 2-14 year age group and 56.4% (95% CI 53.1, 59.6%) among the 15-80 year age group (Zambrana et al., 2018; Balmaseda et al., 2017). The observed post-outbreak seroprevalence in adults is in line with findings from seroprevalence studies from French Polynesia, Brazil, and Bolivia (Aubry et al., 2017; Netto et al., 2017; Saba Villarroel et al., 2018).

In this study, we used data from the 2016 ZIKV epidemic in Managua and developed an agent-based model (ABM) to predict the evolution of age-specific protective immunity to ZIKV infection in the population of Managua, Nicaragua during the period 2017-2097. We assessed: 1) the risk of a future ZIKV outbreak; 2) the effects of a future ZIKV outbreak on women of reproductive age; 3) the influence of loss of immunity on future attack rates; and 4) how vaccination could prevent future ZIKV outbreaks.

2 Methods

2.1 Modelling strategy

We assessed the consequences of future outbreaks of ZIKV infection in Managua, Nicaragua using a stochastic ABM. The model follows a basic susceptible-infected-recovered (SIR) framework and integrates processes related to ZIKV transmission, immunity, demography, adverse congenital outcomes and vaccination (Table 1). We parametrized the model based on published estimates or

Table 1: Parametrization of the agent-based model. [a]age-dependent parameters; [b]the different scenarios are discussed in the text in detail under the headings corresponding to the headings of this table.

Parameter	Comment	Source
ZIKV epidemic parameters		
Transmission rate[a]	Inferred from the 2016 epidemic	Zambrana et al. (2018)
Recovery rate	Inferred from the 2016 epidemic	Zambrana et al. (2018)
ZIKV immunity		
Initial immunity[a]	Inferred from the 2016 epidemic	Zambrana et al. (2018)
Duration of immunity	Lifelong or decaying with time	5 scenarios[b]
Demography		
Initial age distribution	–	World Bank (2019a)
Birth rate	–	World Bank (2019a)
Death rate[a]	–	World Health Organization (2019)
Ageing	Linear ageing at each time-step	–
ZIKV reintroduction		
Delay until reintroduction	1 to 80 years	80 scenarios[b]
Cases reintroduced	1, 5 or 10 cases	3 scenarios[b]
Risk of adverse congenital event		
Exposure	Proportion of women in the first semester of pregnancy	World Bank (2019a)
Risk of microcephaly	Upon infection during exposure time (3 levels of risk)	Cauchemez et al. (2016); Johansson et al. (2016)
Targeted vaccination		
Date of implementation	In 2021, 2025 or 2031	3 scenarios[b]
Effective coverage	Proportion of 15 year old girls vaccinated (0% to 80%)	5 scenarios[b]

inferences from data about the 2016 ZIKV epidemic (Table 1). We considered different scenarios about the duration of immunity, the timing and scale of ZIKV reintroductions in the population, and the timing and scale of a hypothetical vaccination program targeted towards 15 year old girls.

2.2 Model structure

We simulated a population of 10,000 individuals for 80 years (2017–2097). We assigned agents age and ZIKV infection status (susceptible S, infected I or immune R). Initial conditions reflect the situation in Managua, Nicaragua in 2017, when there was no documentation of active transmission. In the outbreak-free period, we only considered demographic and immunity processes: births, deaths, ageing and, if applicable, loss of immunity and vaccination. Given the scarcity of these events at the individual level, we select a long time-step of seven days and stochastically evaluated the epidemic-related transition probabilities at each time step for each agent. After a given time, ZIKV cases were reintroduced in the population. Upon reintroduction, the time step was reduced to 0.1 days, and we evaluated the transition probabilities. Susceptible agents may become infected at a rate $\beta_a I/N$, where β_a is the age-dependent transmission rate and N the total population size. We ignored the vector population and assumed that the force of infection is proportional to the overall infection prevalence. We allowed six months for the outbreak to finish after introduction. Simulations were conducted independently for each combination of scenarios and repeated 1,000

times. In the baseline scenario, we assumed no vaccination, no loss of immunity and an introduction of 10 infected individuals per simulation.

We implemented the model in 'Stan' version 2.18 (Carpenter et al., 2017) and we conducted analyses with R version 3.5.1 (R Core Team and Team, 2008). The Bayesian inference framework Stan permits the use of probability distributions over parameters instead of single values, allowing for the direct propagation of uncertainty. Stan models are compiled in C++, which improves the efficiency of simulations. Algorithm 1 (Appendix A.1) describes the ABM in pseudo code. The model code and data are available from `http://github.com/ZikaProject/SeroProject`.

2.3 Parametrization

2.3.1 ZIKV epidemic parameters

We inferred the probability distributions for the age-specific transmission rate β_a and the recovery rate γ from data on the 2016 ZIKV epidemic in Managua, Nicaragua. We used surveillance data (Zambrana et al., 2018), which give weekly numbers of incident ZIKV infections, confirmed by RT-PCR (dataset $\mathbb{A}$), and survey data on age-stratified ZIKV seroprevalence, measured among participants of pediatric and household cohort studies in Managua during weeks 5–32 of 2017 (dataset $\mathbb{B}$, n=3,740 children and 1,074 adults) (Zambrana et al., 2018).

We conducted statistical inference using a deterministic, ordinary differential equation (ODE)-based version of the ABM with three compartments (S, I and R) and two age classes ($a \in \{1, 2\}$ corresponding to ages 0–14 and ≥15):

$$\frac{dS_a}{dt} = -\beta_a S_a \frac{\sum I_a}{N} \tag{1}$$

$$\frac{dI_a}{dt} = \beta_a S_a \frac{\sum I_a}{N} - \gamma I_a \tag{2}$$

$$\frac{dR_a}{dt} = \gamma I_a \tag{3}$$

We ignored demography in this model because it covers a short time span. We recorded the overall cumulative incidence of ZIKV cases using a dummy compartment:

$$\frac{dC}{dt} = \sum_a \beta_a S_a \frac{\sum I_a}{N} \tag{4}$$

in order to compute the weekly incidence on week t:

$$D_t = C(t) - C(t-1) \tag{5}$$

We fitted the model to weekly incidence data $\mathbb{A}$ using a normal likelihood after a square-root variance-stabilizing transformation (Guan, 2009):

$$\Pr(\mathbb{A}|\beta_a, \gamma, \rho, \sigma) = \prod_t \mathcal{N}(\sqrt{\mathbb{A}}|\sqrt{\rho D}, \sigma) \tag{6}$$

where ρ is a reporting rate parameter and σ an error parameter. In addition, we also fitted the model to the number of individuals with anti-ZIKV antibodies at the end of the epidemic by age group $\mathbb{B}_a$ using a binomial likelihood:

$$\Pr(\mathbb{B}|\beta_a, \gamma) = \prod_a \mathcal{B}(\mathbb{B}_a|n_a, p_a) \tag{7}$$

where $\mathbb{B}_a$ the number of individuals with antibodies, n_a is the number of individuals in each age group, and $p_a = R_a(t_{end})/N_a(t_{end})$ the proportion of immune at the end of the epidemic. The

full likelihood was obtained by multiplying Eq. 6 and Eq. 7. We chose weakly-informative priors for all parameters and fitted the model in Stan (Table 2). We describe the calculation of the basic reproduction number $\mathcal{R}_0$ in appendix A.2. We used one thousand posterior samples for β_a and γ obtained by Hamiltonian Monte Carlo in the ABM model, ensuring the full propagation of uncertainty. Parameter values can translate from deterministic to agent-based versions of an epidemic model if the time step is small (Roche et al., 2011a), which was the reason for using a time step of 0.1 days.

Table 2: Parameter estimates inferred from incidence and sero-prevalence data on the 2016 ZIKV epidemic in Managua, Nicaragua. CrI: Credible interval.

Parameter	Interpretation	Prior	Posterior (median and 95% CrI)
β_1	Transmission for age group 0-14	Expon(0.1)	0.19 (0.16; 0.22)
β_2	Transmission for age group $\geq$15	Expon(0.1)	0.32 (0.30; 0.36)
$1/\gamma$	Duration of infectious period	Gamma$(1, 0.1)$	4.8 (4.3; 5.4)
ρ	Reporting rate	Beta$(1, 1)$	0.24% (0.21; 0.26)
$I(0)$	Initial number of infectious	Expon(0.1)	74 (40; 134)
$\mathcal{R}_0$	Basic reproduction number	–	1.58 (1.56; 1.59)

2.3.2 ZIKV immunity

We used the deterministic model, described in the previous section, to infer the proportion of people with protective immunity within each age group at the end of the 2016 epidemic $\tilde{p}_a$. We used one thousand posterior samples of $\tilde{p}_a$ in the ABM to allow the propagation of uncertainty. Protective immunity to ZIKV after infection was lifelong in our first scenario, so the reduction of the overall proportion of immune individuals in the population decreased only because of population renewal. Given the absence of evidence about the duration of immunity to ZIKV, we considered four scenarios assuming exponentially distributed durations of immunity with means of 30, 60, 90, or 150 years. These values correspond to a proportion of initially immune agents that loses immunity after 10 years of 28%, 15%, 11% or 6%, respectively (Appendix A.3).

2.3.3 Demography

We based the initial age distribution of the population on data from the World Bank (World Bank, 2019b). We used age-dependent death rates for 2016 from the World Health Organization (WHO) (World Health Organization, 2019). For births, we computed a rate based on the average birth rate in Nicaragua of 2.2 births per woman, which was uniformly distributed over the female reproductive lifespan (World Bank, 2019a). We defined the period of reproductive age between 15 and 49 years. Ageing is linear, increasing the age of each agent by 7 days at each 7-day time step.

2.3.4 ZIKV reintroduction

We reintroduced ZIKV in the population after a delay of $d = \{1, \cdots, 80\}$ years in independent simulations. We chose this approach rather than continuous reintroductions to remove some of the stochasticity and assess more clearly the association between immunity decay and risk of an outbreak. As the probability of an extinction of the outbreak depends on the number of ZIKV cases reintroduced in the population, we considered three different values for the seed (1, 5 or 10 cases) and compared the results (Appendix A.4). Simulations using continuous reintroductions each year are presented in the appendix A.5.

2.3.5 Risk of adverse congenital outcomes

The estimated number of microcephaly cases resulting from the reintroduction of ZIKV depended on the exposure, i.e. the number of pregnant women infected by ZIKV during their first trimester, to which we applied three different levels of risk, based on published estimates (Cauchemez et al., 2016; Johansson et al., 2016). We obtained the number of ZIKV infections among women aged 15–49 years from ABM simulations. As gender was not explicitly considered in the model, we assumed that women represented 50% of the population. We assumed a uniform distribution of births during the reproductive period, and considered that the first trimester constituted a third of ongoing pregnancies at a given time. We explored three different levels of risk of microcephaly in births to pregnant woman with ZIKV infection during the first trimester, as reported by Zhang et al., based on data from French Polynesia (0.95%, called low risk) and Brazil (2.19% and 4.52%, called intermediate and high risk, respectively) (Cauchemez et al., 2016; Johansson et al., 2016).

2.3.6 Vaccination

We examined the effects of a potential ZIKV vaccine, given to 15-year-old-girls. This vaccination strategy was used for rubella virus, which also causes congenital abnormalities, before the vaccine was included in the measles, mumps and rubella vaccine given in childhood (Vyse et al., 2002). The main objective of vaccination would be the prevention of adverse congenital outcomes, including microcephaly. We simulated this intervention in the ABM, assuming vaccine implementation starting in 2021, 2025 or 2031. From that date, half of the agents reaching age 15, representing females, could transition to immune status R with various effective vaccination coverage (from 20% to 80%).

2.4 Outcome analysis

From the simulations, we collected 1) the evolution of the age-specific ZIKV immunity in the population; 2) the attack rate resulting from the reintroduction of ZIKV at year d; 3) the age of newly infected individuals. We fitted a binary Gaussian mixture model to dichotomize the observed attack rates into either outbreaks or non-outbreaks. We defined the outbreak threshold as the 97.5% upper bound of the lower distribution. This corresponded to a threshold of 1%, so that attack rates $\geq$1% were considered as outbreaks. The age structure of newly infected individuals was used to compute relative risks of infection by age group.

3 Results

3.1 2016 ZIKV epidemic

The fitted model (Figure 1), resulted in a reporting rate of 0.24% (95% credible interval, CrI: 0.21; 0.26) and a transmission rate of 42% (95% CrI: 35-48) lower for the 0–14 age group than in the $\geq$15 age group. This corresponded to an overall basic reproduction number $\mathcal{R}_0$ of 1.58 (95% CrI: 1.56; 1.59). The predicted percentage of immune at the end of the epidemic was 36% (95% CrI: 34;38) for the 0–14 age group and 53% (95% CrI: 50;57) for the $\geq$15 age group.

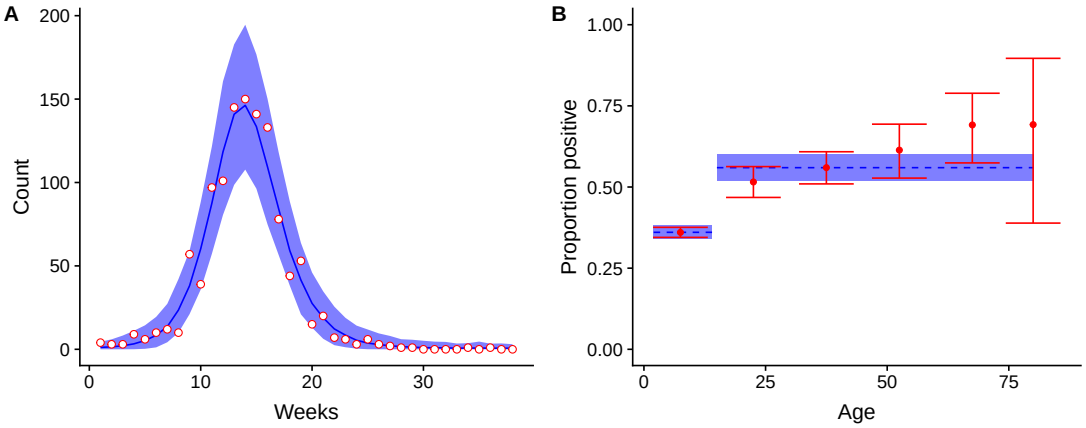

Figure 1: Model fit for (A) weekly incidence data and (B) post-epidemic sero-prevalence data from the 2016 ZIKV epidemic in Managua, Nicaragua. Data points are in red and the corresponding model fit (posterior median and 95% credible interval) is in blue.

3.2 Immunity and population

In our simulation, the expected population size increased by 42% between 2017 and 2097. Under the assumption that ZIKV infection results in lifelong protective immunity, population renewal will create an imbalance in the proportion immune in different age groups. We expect the overall proportion of protective immunity in the population to have halved (from 48% to 24%) by 2051 and to be concentrated among the older age classes (Fig. 2A). The 0–14 year old age group will become entirely susceptible by 2031 and the 15–29 year old age group by 2046.

3.3 Future risk of ZIKV outbreak

Reintroductions of ZIKV in the population of Managua are unlikely to develop into sizeable outbreaks before 2040, 24 years after the 2016 epidemic, assuming lifelong immunity for those infected (Fig. 2B). After this point, attack rates resulting from ZIKV reintroduction will rise steeply. By 2047, we predict that ZIKV reintroductions will have a 50% probability of resulting in outbreaks with attack rates greater than 1% (Fig. 2C).

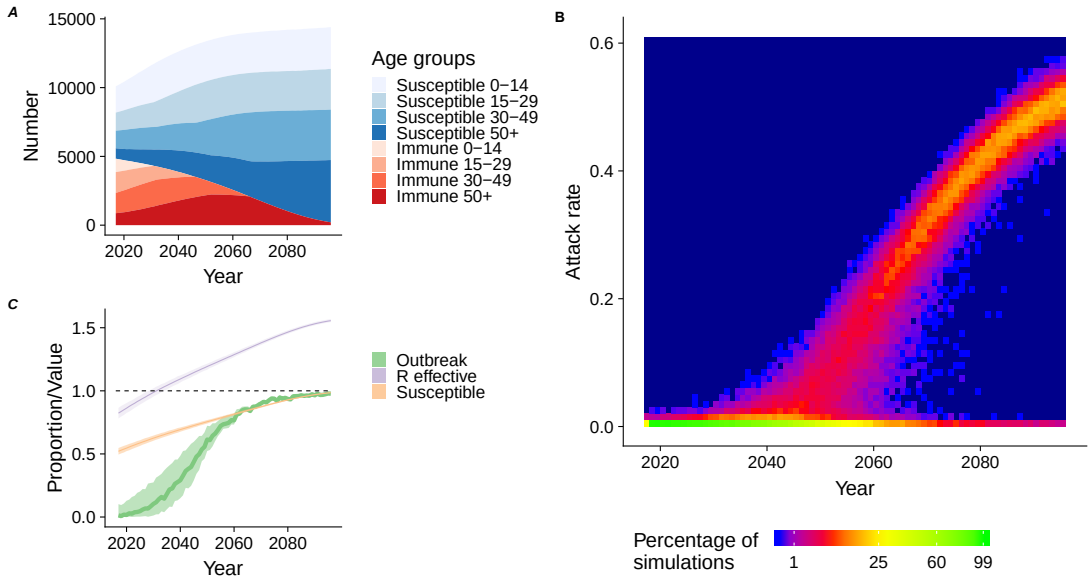

Figure 2: (A) The evolution of the immunity status per age group in a population of 10,000 agents for the next 80 years based on the demographic structure of Nicaragua. (B) Heat map of the distribution of the attack rates resulting from the reintroduction of ZIKV in the population at each year (1000 simulations for each year). (C) The evolution of the proportion of reintroductions resulting in outbreaks (with a threshold of 1%) with time (green), proportion of susceptible (orange), and effective reproduction number $\mathcal{R}_e$ (purple).

3.4 Risk of infection and microcephaly births in women of reproductive age

The differences between age groups in both immunity and transmission will result in a disproportionate burden of infection in the 15–29 age class. The relative risk of infection in this age group ranges from 1.2 to 1.6, compared with the general population if an outbreak occurs during the period 2032–2075 (Fig. 3A). Most pregnancies occur in this age group, so these women are also the most likely to experience a pregnancy with an adverse outcome. The increased risk of infection in this group implies that the number of adverse congenital outcomes resulting from a ZIKV outbreak during this period is likely to be higher than expected with a homogeneous distribution of immunity across ages. Assuming different values for the added risk of microcephaly after a ZIKV infection during the first trimester, we expect the mean number of microcephaly cases due to ZIKV infection resulting from the reintroduction of ZIKV in Managua, Nicaragua to reach 1 to 5 cases per 100,000 population in 2060 (Fig. 3B).

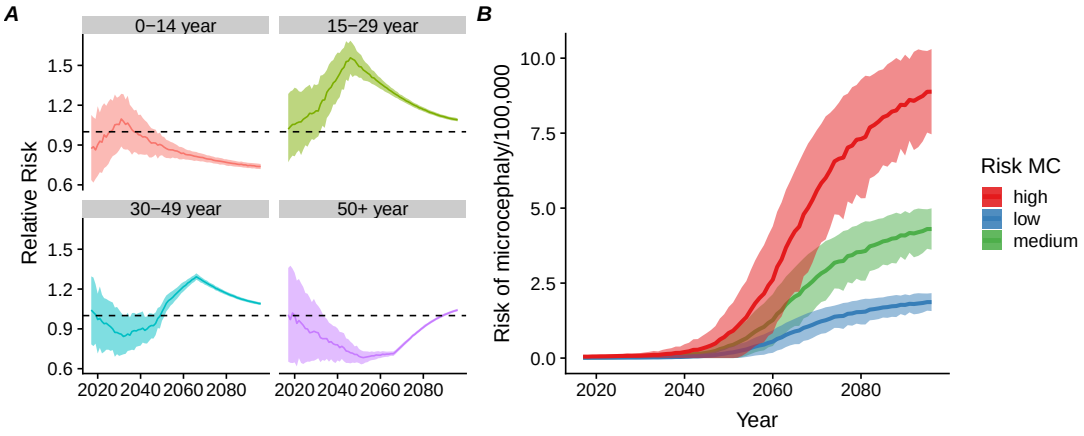

Figure 3: (A) Relative risk of ZIKV infection during a ZIKV outbreak per age group compared to the general population by year (median, interquartile range). (B) Expected number of additional microcephaly events associated with ZIKV infection during pregnancy per 100,000 total population according to three different risk scenarios.

3.5 Loss of immunity

If protective immunity to ZIKV is not lifelong, the window before observing a rise in the attack rates resulting from ZIKV reintroduction will shorten (Fig. 4A). For instance, if 15% of the those who were infected in 2016 lose their immunity after 10 years (a mean duration of immunity of 60 years), the time until the risk of outbreak upon reintroduction reaches 50% would be 16 years earlier (2031) than with lifelong immunity (2047). Loss of immunity over time would reduce the relative risk in the 15–29 year old age group (Fig. 4B).

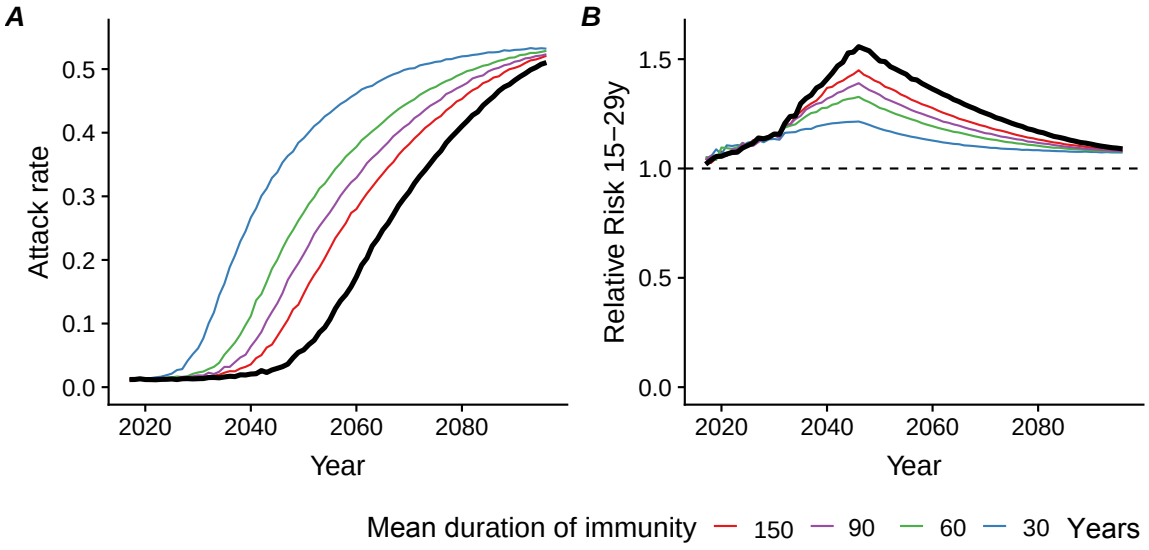

Figure 4: Consequences of alternative scenarios regarding the mean duration of protective immunity (30, 60 and 150 years), compared with lifelong immunity (thick black line): (A) median attack rate of ZIKV among reintroductions resulting in outbreaks (with a threshold of 1%) and (B) relative risk of ZIKV infection during an outbreak in the 15–29 year age group compared with the general population.

3.6 Targeted vaccination

The implementation of a vaccination program targeted towards 15 year old girls between 2021 and 2031 would reduce the risk of infection in women aged 15-29 years and would also reduce the overall risk of a ZIKV outbreak in the population (Fig. 5). If effective vaccine coverage is 60–80% amongst 15 year old girls, the prolongation of herd immunity could effectively mitigate the overall risk of a ZIKV outbreak in the population. The reduction in the number of microcephaly cases would then exceed what would be expected by considering only the direct protection granted by a vaccine to future mothers. A later implementation of the intervention would be less effective, as it becomes more difficult to maintain the herd immunity (Figure 5B).

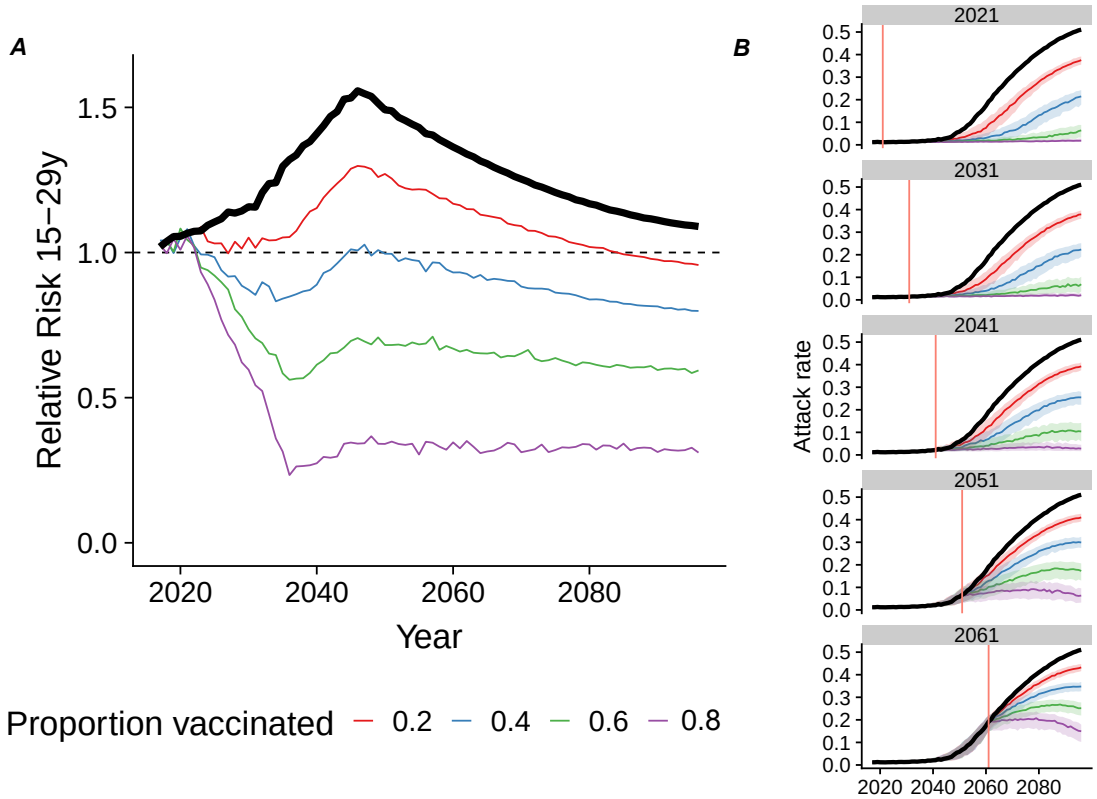

Figure 5: Consequences of implementing a targeted vaccination program among 15-year-old-girls from 2021 onwards with various levels of effective vaccination coverage (from 20 to 80%) compared with no vaccination (thick black line): (A) relative risk of ZIKV infection during an outbreak in the 15–29 year age group compared with the general population and (B) attack rate of ZIKV among reintroductions resulting in outbreaks (median, interquartile range, with a threshold of 1%), when vaccination is introduced from 2021, 2031, 2041, 2051 or 2061 onwards (red vertical line).

4 Discussion

In this mathematical modeling study, we show that a new ZIKV outbreak in Nicaragua would affect proportionally more the women in the young reproductive age range (15-29 years), owing to the age-dependent infection pattern and population renewal. The risk of a new ZIKV outbreak in Nicaragua, after reintroduction, will remain low before 2035 because of herd immunity, then rise to 50% in 2047. If protective immunity to ZIKV decays with time, which remains to be elucidated, ZIKV recurrence could occur sooner; in that case, the distribution of the risk would be more equal across age groups. Targeted vaccination, focusing on females aged 15 years would both reduce the risk of adverse congenital outcomes and extend herd immunity, mitigating the overall risk of an outbreak and resulting in lower attack rates if an outbreak occurred.

4.1 Modelling choices

We used an ABM to predict the future risk of ZIKV outbreak because of the stochastic nature of outbreak emergence upon reintroduction of a few infectious cases in a population. ABMs can also

model the linear process of ageing realistically, whereas an ODE-based model including different compartments for each age group would incorrectly consider exponential time distributions between successive classes. Parametrization of the ABM was based on data on incidence and post-epidemic seroprevalence for the 2016 ZIKV epidemic in Managua, Nicaragua, fitted with a deterministic, ODE-based model. A strength of our approach is that it allows for the full propagation of uncertainty from the initial data into the risk assessment, by transferring the parameter distributions from the ODE model to the ABM. Roche et al. showed that, when a sufficiently small time step was chosen, stochastic and deterministic models using the same parameter values led to similar results (Roche et al., 2011b).

We chose a simple SIR structure, as used by Netto et al., focusing on the dynamics of infection and immunity in the human population and not modeling vector populations and behavior, as in some other studies (Kucharski et al., 2016; Champagne et al., 2016; Ferguson et al., 2016). This simplification limits the mechanistic interpretation of the epidemic parameters, but the primary aim of our model was to provide a phenomenological description of the transmission dynamics. Given our main objective, which was to determine the risk of an outbreak after reintroduction of ZIKV, is mostly influenced by the level of protective immunity in the human population, this approach is appropriate. Of course, the future occurrence of ZIKV in the area also depends on the presence of a competent vector. Our choice is supported by sensitivity analyses that show that more complex model structures (delayed SIR and Ross-MacDonald-type models) were not superior to a simple SIR structure in describing the 2016 ZIKV epidemic of Managua (Appendix A.6). Similarly, Pandey et al. (2013) showed that additional model complexity does not result in a better description of the dynamics of transmission of dengue virus (another Aedes-borne virus) in a human population compared with an SIR model (Pandey et al., 2013).

4.2 Comparison with other models

We found a $\mathcal{R}_0$ of 1.58 for the 2016 ZIKV epidemic in Managua; other estimates of $\mathcal{R}_0$ vary, ranging from 1.4-1.7 for the French West Indies, 1.9-2.2 for French Polynesia, 2.1 for Salvador Brazil to 4.3-5.8 for Yap Island (Champagne et al., 2016; Kucharski et al., 2016; Nishiura et al., 2016; Riou et al., 2017). The variation can be attributed to differences in methods and settings. Our comparatively low estimate for $\mathcal{R}_0$ was obtained using the seroprevalence observed in Nicaragua after the ZIKV epidemic. If the epidemic stopped because of a lack of susceptible individuals, the proportion of immune in a homogeneous mixed population has to be at least $1-1/\mathcal{R}_0$ (Dietz, 1975). $\mathcal{R}_0$ values ranging between 1.5 and 3 are in line with post-epidemic seroprevalence levels of 33-67%, as observed here. Other analyses, based on incidence data only, resulted in higher $\mathcal{R}_0$ values and predicted very high post-epidemic seroprevalence levels, e.g. 87-97% in (Kucharski et al., 2016), which were contradicted by later seroprevalence studies (49% observed (Aubry et al., 2017)). Other authors dealt with this discrepancy by removing the assumption of homogeneous mixing, allowing for a proportion of the population to be excluded from participating in the epidemic (Champagne et al., 2016).

Several authors have studied the time to a next ZIKV outbreak. Our estimates of the time until the risk increases, are similar to the 12-20 years before re-emergence, as estimated for French Polynesia (Kucharski et al., 2016). The advantage of our study is that we show the age-stratified impact of a new ZIKV outbreak, based on different attack rates for children and adults. Netto et al (2017) used a SEIR model to show that in Salvador, Brazil, the effective reproduction number was insufficient to cause a new outbreak during the "subsequent years" (Netto et al., 2017). Lourenço (2017) showed the same for the whole of Brazil: herd immunity should protect the population from a new outbreak in the coming years (Netto et al., 2017). Ferguson et al. (2016) concluded that the age distribution of future ZIKV outbreaks will likely differ and that a new large epidemic will be delayed for "at least a decade", (Ferguson et al., 2016). Our work, which models the processes of ageing in relation to protective immunity to ZIKV explicitly, provides a quantified confirmation of

these previous works, but adds the effect of different transmission rates by age group.

4.3 Targeted vaccination

The benefits of a new ZIKV vaccine in reducing the risk of new outbreaks and of further epidemics of adverse congenital outcomes depend on timing. A ZIKV vaccine that is available between 2021-2031 would not only protect vaccinated women from adverse congenital outcomes, but also provide indirect protection to unvaccinated women and more generally to the whole population by extending herd immunity. Phase I clinical trials of ZIKV candidate vaccines have shown levels of neutralizing antibody titers that were considered protective against reinfection (Gaudinski et al., 2018; Modjarrad et al., 2018). Some vaccines have already entered phase II trials (National Institute of Allergy and Infectious Diseases, 2018). But, there are substantial obstacles to vaccine licensure. First, the evaluation of vaccine efficacy has stalled because the reduced circulation of ZIKV has reduced the visibility of ZIKV-associated disease (Cohen, 2018). Second, it remains unclear if neutralizing antibodies induced by vaccination are sufficient to protect women against vertical transmission and congenital abnormalities (Diamond et al., 2018). Third, it is not clear whether or how vaccine-induced antibodies against ZIKV will cross-react with other flaviviruses.

4.4 Conceptual limitations

In our model, we did not take migration into account. An influx of people with lower levels of protective immunity or higher birth rates would increase the speed at which the population becomes susceptible again. Nicaragua has an urbanization rate that exceeds the world average (Maria et al., 2017). If rural populations have lower seroprevalence for ZIKV, as was shown in Suriname (Langerak et al., 2019), an inflow of rural inhabitants into Managua could increase the risk of ZIKV outbreaks. Uncertainty remains, as factors such as political instability can drive migration and influence disease transmission, as we currently observe in Venezuela and bordering countries (Tuite et al., 2018).

Vector densities are likely to change over time. Here, we assumed a constant transmission rate, as observed in the 2016 outbreak. This transmission rate (β_a), captures both human-mosquito and mosquito-human transmission. Mosquito distributions change in space and time and are influenced by environmental changes (Campbell et al., 2015). Due to climate change, globally, we expect to see an expansion of their habitat (Kraemer et al., 2019). However, we know that mosquitoes adapt to new conditions by, for example, changing their behavior. Chadee et al. (2016) observed a shift of *Aedes* mosquitoes to cooler underground sources of water as a result of warming of their habitat (Chadee and Martinez, 2016).

The generalizability of some conclusions is limited. ZIKV has touched most tropical regions of the Americas. In many of these regions, ZIKV epidemics resulted in a high post-epidemic seroprevalence, similar to Nicaragua. However, differences in vector density and demography limit the scope and generalizability of our predictions regarding the time until ZIKV recurrence. Conversely, the increased burden experienced by younger age groups and the subsequent higher-than-expected number of adverse congenital events resulting from a ZIKV outbreak is likely to hold in many settings. Seroprevalence studies across the Americas in all age strata, using tests with high specificity, would greatly help risk prediction.

4.5 Conclusion

Preparedness is vital; the time until the next outbreak gives us to opportunity to be prepared. The next sizeable ZIKV outbreak in Nicaragua will likely not occur before 2040 but the probability of outbreaks will increase. Young women of reproductive age will be at highest risk of infection during the next ZIKV outbreak. Vaccination targeted to young women could curb the risk of a large outbreak and extend herd immunity. ZIKV vaccine development and licensure are urgent to

attain the maximum benefit in reducing the population-level risk of infection and the risk of adverse congenital outcomes.

5 Acknowledgments

Calculations were performed on UBELIX (`http://www.id.unibe.ch/hpc`), the HPC cluster at the University of Bern. MJC received salary support from the Swiss National Science Foundation (project grant 320030_176233).

6 Competing interests

References

Abbink P, Stephenson KE, Barouch DH. Zika virus vaccines. Nat Rev Microbiol. 2018; 16(10):594–600. doi: 10.1038/s41579-018-0039-7.

Aubry M, Teissier A, Huart M, Merceron S, Vanhomwegen J, Roche C, Vial AL, Teururai S, Sicard S, Paulous S, Desprès P, Manuguerra JC, Mallet HP, Musso D, Deparis X, Cao-Lormeau VM. Ross river virus seroprevalence, French Polynesia, 2014–2015. Emerg Infect Dis. 2017; 23(10):1751–1753. doi: 10.3201/eid2310.170583.

Balmaseda A, Stettler K, Medialdea-Carrera R, Collado D, Jin X, Zambrana JV, Jaconi S, Cameroni E, Saborio S, Rovida F, Percivalle E, Ijaz S, Dicks S, Ushiro-Lumb I, Barzon L, Siqueira P, Brown DWG, Baldanti F, Tedder R, Zambon M, et al. Antibody-based assay discriminates Zika virus infection from other flaviviruses. Proc Natl Acad Sci. 2017; 114(31):8384–8389. doi: 10.1073/pnas.1704984114.

Campbell LP, Luther C, Moo-Llanes D, Ramsey JM, Danis-Lozano R, Peterson AT. Climate change influences on global distributions of dengue and chikungunya virus vectors. Philos Trans R Soc B Biol Sci. 2015; 370(1665):1–9. doi: 10.1098/rstb.2014.0135.

Cao-Lormeau VM, Roche C, Teissier A, Robin E, Berry AL, Mallet HP, Sall AA, Musso D. Zika Virus, French Polynesia, South Pacific, 2013. Emerg Infect Dis. 2014; 20(6):1085. doi: 10.3201/eid2006.140138.

Carpenter B, Gelman A, Hoffman MD, Lee D, Goodrich B, Betancourt M, Brubaker M, Guo J, Li P, Riddell A. Stan : A Probabilistic Programming Language. J Stat Softw. 2017; 76(1). doi: 10.18637/jss.v076.i01.

Cauchemez S, Besnard M, Bompard P, Dub T, Guillemette-Artur P, Eyrolle-Guignot D, Salje H, Van Kerkhove MD, Abadie V, Garel C, Fontanet A, Mallet HP. Association between Zika virus and microcephaly in French Polynesia, 2013-15: A retrospective study. Lancet. 2016; 387(10033):2125–2132. doi: 10.1016/S0140-6736(16)00651-6.

Chadee DD, Martinez R. Aedes aegypti (L.) in Latin American and Caribbean region: With growing evidence for vector adaptation to climate change? Acta Trop. 2016 apr; 156:137–143. doi: 10.1016/j.actatropica.2015.12.022.

Champagne C, Salthouse DG, Paul R, Cao-Lormeau VM, Roche B, Cazelles B. Structure in the variability of the basic reproductive number (R0) for Zika epidemics in the Pacific islands. Elife. 2016 nov; 5(NOVEMBER2016). doi: 10.7554/eLife.19874.

Cohen J. Steep drop in Zika cases undermines vaccine trial. Science. 2018; 361(6407):1055–1056. doi: 10.1126/science.361.6407.1055.

Counotte MJ, Egli-Gany D, Riesen M, Abraha M, Porgo TV, Wang J, Low N. Zika virus infection as a cause of congenital brain abnormalities and Guillain-Barré syndrome: From systematic review to living systematic review. F1000Research. 2018; 7(196):196. doi: 10.12688/f1000research.13704.1.

Diamond MS, Ledgerwood JE, Pierson TC. Zika Virus Vaccine Development: Progress in the Face of New Challenges. Annu Rev Med. 2018; 70(1):121–135. doi: 10.1146/annurev-med-040717-051127.

Diekmann O, Heesterbeek JAP, Roberts MG. The construction of next-generation matrices for compartmental epidemic models. J R Soc Interface. 2010; 7(47):873–885. doi: 10.1098/rsif.2009.0386.

Dietz K. Transmission and control of arbovirus diseases. Epidemiology. 1975; 104:104–121.

Duffy MR, Chen TH, Hancock WT, Powers AM, Kool JL, Lanciotti RS, Pretrick M, Marfel M, Holzbauer S, Dubray C, Guillaumot L, Griggs A, Bel M, Lambert AJ, Laven J, Kosoy O, Panella A, Biggerstaff BJ, Fischer M, Hayes EB. Zika Virus Outbreak on Yap Island, Federated States of Micronesia. N Engl J Med. 2009; 360(24):2536–2543. doi: 10.1056/NEJMoa0805715.

Faria NR, Do Socorro Da Silva Azevedo R, Kraemer MUG, Souza R, Cunha MS, Hill SC, Thézé J, Bonsall MB, Bowden TA, Rissanen I, Rocco IM, Nogueira JS, Maeda AY, Da Silva Vasami FG, De Lima Macedo FL, Suzuki A, Rodrigues SG, Cruz ACR, Nunes BT, De Almeida Medeiros DB, et al. Zika virus in the Americas: Early epidemiological and genetic findings. Science. 2016; 352(6283):345–349. doi: 10.1126/science.aaf5036.

Ferguson NM, Cucunubá ZM, Dorigatti I, Nedjati-Gilani GL, Donnelly CA, Basáñez MG, Nouvellet P, Lessler J. Countering the Zika epidemic in Latin America. Science. 2016; 353(6297):353–354. doi: 10.1126/science.aag0219.

Gaudinski MR, Houser KV, Morabito KM, Hu Z, Yamshchikov G, Rothwell RS, Berkowitz N, Mendoza F, Saunders JG, Novik L, Hendel CS, Holman LSA, Gordon IJ, Cox JH, Edupuganti S, McArthur MA, Rouphael NG, Lyke KE, Cummings GE, Sitar S, et al. Safety, tolerability, and immunogenicity of two Zika virus DNA vaccine candidates in healthy adults: randomised, open-label, phase 1 clinical trials. Lancet. 2018; 391(10120):552–562. doi: 10.1016/S0140-6736(17)33105-7.

Guan Y. Variance stabilizing transformations of Poisson, binomial and negative binomial distributions. Stat Probab Lett. 2009; 79(14):1621–1629. doi: 10.1016/j.spl.2009.04.010.

Haby MM, Pinart M, Elias V, Reveiz L. Prevalence of asymptomatic Zika virus infection: A systematic review. Bull World Health Organ. 2018; 96(6):402–413D. doi: 10.2471/BLT.17.201541.

Henderson AD, Aubry M, Kama M, Vanhomwegen J, Teissier A, Mariteragi-Helle T, Paoaafaite T, Manuguerra JC, Edmunds WJ, Whitworth J, Watson CH, Lau CL, Cao-Lormeau VM, Kucharski AJ. Zika virus seroprevalence declines and neutralization antibodies wane in adults following outbreaks in French Polynesia and Fiji. bioRxiv. 2019; p. 578211. `http://biorxiv.org/content/early/2019/03/15/578211.abstract`, doi: 10.1101/578211.

Johansson MA, Mier-Y-Teran-Romero L, Reefhuis J, Gilboa SM, Hills SL. Zika and the risk of Microcephaly. Obstet Gynecol Surv. 2016; 71(11):635–636. doi: 10.1097/OGX.0000000000000386.

Kohl A, Gatherer D. Zika virus: a previously slow pandemic spreads rapidly through the Americas. J Gen Virol. 2015; 97(2):269–273. doi: 10.1099/jgv.0.000381.

Kraemer MUG, Reiner RC, Brady OJ, Messina JP, Gilbert M, Pigott DM, Yi D, Johnson K, Earl L, Marczak LB, Shirude S, Davis Weaver N, Bisanzio D, Perkins TA, Lai S, Lu X, Jones P, Coelho GE, Carvalho RG, Van Bortel W, et al. Past and future spread of the arbovirus vectors Aedes aegypti and Aedes albopictus. Nat Microbiol. 2019; 4(5):854–863. doi: 10.1038/s41564-019-0376-y.

Krauer F, Riesen M, Reveiz L, Oladapo OT, Martínez-Vega R, Porgo TV, Haefliger A, Broutet NJ, Low N. Zika Virus Infection as a Cause of Congenital Brain Abnormalities and Guillain–Barré Syndrome: Systematic Review. PLoS Med. 2017; 14(1):e1002203. doi: 10.1371/journal.pmed.1002203.

Kucharski AJ, Funk S, Eggo RM, Mallet HP, Edmunds WJ, Nilles EJ. Transmission Dynamics of Zika Virus in Island Populations: A Modelling Analysis of the 2013–14 French Polynesia Outbreak. PLoS Negl Trop Dis. 2016; 10(5):e0004726. doi: 10.1371/journal.pntd.0004726.

Langerak T, Brinkman T, Mumtaz N, Arron G, Hermelijn S, Baldewsingh G, Wongsokarijo M, Resida L, Rockx B, Koopmans MPG, Van Gorp ECM, Vreden S. Zika Virus Seroprevalence in Urban and Rural Areas of Suriname, 2017. J Infect Dis. 2019; doi: 10.1093/infdis/jiz063.

Maria A, Acero JL, Aguilera AI, Lozano MG. Central America Urbanization Review: Making Cities Work for Central America. The World Bank; 2017. doi: 10.1596/978-1-4648-0985-9.

Modjarrad K, Lin L, George SL, Stephenson KE, Eckels KH, De La Barrera RA, Jarman RG, Sondergaard E, Tennant J, Ansel JL, Mills K, Koren M, Robb ML, Barrett J, Thompson J, Kosel AE, Dawson P, Hale A, Tan CS, Walsh SR, et al. Preliminary aggregate safety and immunogenicity results from three trials of a purified inactivated Zika virus vaccine candidate: phase 1, randomised, double-blind, placebo-controlled clinical trials. Lancet. 2018; 391(10120):563–571. doi: 10.1016/S0140-6736(17)33106-9.

National Institute of Allergy and Infectious Diseases, VRC 705: A Zika Virus DNA Vaccine in Healthy Adults and Adolescents (DNA); 2018. [Online]. Available from: `https://clinicaltrials.gov/ct2/show/NCT03110770`.

Netto EM, Moreira-Soto A, Pedroso C, Höser C, Funk S, Kucharski AJ, Rockstroh A, Kümmerer BM, Sampaio GS, Luz E, Vaz SN, Dias JP, Bastos FA, Cabral R, Kistemann T, Ulbert S, de Lamballerie X, Jaenisch T, Brady OJ, Drosten C, et al. High Zika Virus Seroprevalence in Salvador, Northeastern Brazil Limits the Potential for Further Outbreaks. MBio. 2017; 8(6). doi: 10.1128/mbio.01390-17.

Nishiura H, Kinoshita R, Mizumoto K, Yasuda Y, Nah K. Transmission potential of Zika virus infection in the South Pacific. Int J Infect Dis. 2016; 45:95–97. doi: 10.1016/j.ijid.2016.02.017.

PAHO, PAHO - Cumulative Incidence; 2019. [Online]. Available from: `https://www.paho.org/hq/index.php?option=com_content&view=article&id=12390:zika-cumulative-cases&Itemid=42090&lang=en`.

Pandey A, Mubayi A, Medlock J. Comparing vector-host and SIR models for dengue transmission. Math Biosci. 2013; 246(2):252–259. doi: 10.1016/j.mbs.2013.10.007.

R Core Team, Team RDC. R: A Language and Environment for Statistical Computing. Vienna, Austria; 2008.

Riou J, Poletto C, Boëlle PY. A comparative analysis of Chikungunya and Zika transmission. Epidemics. 2017; 19:43–52. doi: 10.1016/j.epidem.2017.01.001.

Roche B, Drake JM, Rohani P. An Agent-Based Model to study the epidemiological and evolutionary dynamics of Influenza viruses. BMC Bioinformatics. 2011; 12(1):87. doi: 10.1186/1471-2105-12-87.

Roche B, Drake JM, Rohani P. An Agent-Based Model to study the epidemiological and evolutionary dynamics of Influenza viruses. BMC Bioinformatics. 2011; 12(1). doi: 10.1186/1471-2105-12-87.

Saba Villarroel PM, Nurtop E, Pastorino B, Roca Y, Drexler JF, Gallian P, Jaenisch T, Leparc-Goffart I, Priet S, Ninove L, de Lamballerie X. Zika virus epidemiology in Bolivia: A seroprevalence study in volunteer blood donors. PLoS Negl Trop Dis. 2018; 12(3):e0006239. doi: 10.1371/journal.pntd.0006239.

Tuite AR, Thomas-Bachli A, Acosta H, Bhatia D, Huber C, Petrasek K, Watts A, Yong JHE, Bogoch II, Khan K. Infectious disease implications of large-scale migration of Venezuelan nationals. J Travel Med. 2018 sep; 25(1). doi: 10.1093/jtm/tay077.

Vyse AJ, Gay NJ, White JM, Ramsay ME, Brown DWG, Cohen BJ, Hesketh LM, Morgan-Capner P, Miller E. Evolution of surveillance of measles, mumps, and rubella in England and Wales: Providing the platform for evidence-based vaccination policy. Epidemiol Rev. 2002; 24(2):125–136. doi: 10.1093/epirev/mxf002.

Wikan N, Smith DR. Zika virus: History of a newly emerging arbovirus. Lancet Infect Dis. 2016; 16(7):e119–e126. doi: 10.1016/S1473-3099(16)30010-X.

World Bank, World Development Indicators; 2019. [Online]. Available from: `https://data.worldbank.org/indicator/SP.DYN.TFRT.IN?locations=NI`.

World Bank, World Development Indicators; 2019. [Online]. Available from: `https://databank.worldbank.org/data/reports.aspx?source=2&series=SP.POP.TOTL.MA.IN&country=NIC`.

World Health Organization. WHO statement on the first meeting of the International Health Regulations (2005) (IHR 2005) Emergency Committee on Zika virus and observed increase in neurological disorders and neonatal malformations. WHO. 2016; .

World Health Organization, WHO Malaria Vaccine Pipeline Tracker; 2018. [Online]. Available from: `https://www.who.int/immunization/research/vaccine_pipeline_tracker_spreadsheet/en/`.

World Health Organization, WHO | By Category | Life Tables by Country - Nicaragua. World Health Organization; 2019. [Online]. Available from: `http://apps.who.int/gho/data/?theme=main&vid=61180`.

Zambrana JV, Bustos Carrillo F, Burger-Calderon R, Collado D, Sanchez N, Ojeda S, Carey Monterrey J, Plazaola M, Lopez B, Arguello S, Elizondo D, Aviles W, Coloma J, Kuan G, Balmaseda A, Gordon A, Harris E. Seroprevalence, risk factor, and spatial analyses of Zika virus infection after the 2016 epidemic in Managua, Nicaragua. Proc Natl Acad Sci. 2018; 115(37):9294–9299. doi: 10.1073/pnas.1804672115.

Zhang Q, Sun K, Chinazzi M, Pastore Y Piontti A, Dean NE, Rojas DP, Merler S, Mistry D, Poletti P, Rossi L, Bray M, Halloran ME, Longini IM, Vespignani A. Spread of Zika virus in the Americas. Proc Natl Acad Sci U S A. 2017; 114(22):E4334–E4343. doi: 10.1073/pnas.1620161114.

Appendices

A Appendix

A.1 ABM algorithm

Here, we provide the pseudo code of the ABM (Algorithm 1).

Algorithm 1 ABM

```
procedure INITIALIZATION                                  ▷ Add initial conditions S/R and sex per n individual
    for n ← 1, popMax do
        R[n] ← select random 1 or 0 with probability(age[n])
        S[n] ← 1 − R[n]
        I[n] ← 0
        sex[n] ← select random 1 or 0 with probability 0.5
    end for
end procedure
procedure SIMULATION                                      ▷ Simulation over wkMax weeks
    for wk ← 1, wkMax do
        for n ← 1, popMax do                              ▷ Loop over popMax individuals
            if individual is alive then
                procedure POPULATION DYNAMICS             ▷ Pre-outbreak
                    Birth, Death, Ageing
                end procedure
                procedure LOSS OF IMMUNITY                ▷ Loss of immunity
                    [R → S] with probability RateToProb(ξ)
                end procedure
                procedure VACCINATION                     ▷ Vaccination
                    [S → R] with probability vaccinationProb, at age[n]
                end procedure
                procedure INFECTION, RECOVERY             ▷ During outbreak
                    [S → I] with probability RateToProb(β, age[n])
                    [I → R] with probability RateToProb(γ)
                end procedure
            end if
        end for
        procedure START OUTBREAK                          ▷ Introduction of infection
            if wk = introductionWk then
                Change timestep: 7 days to 0.1 days
                Collect summary statistics pre-outbreak
                Introduce introductionN infections
            end if
        end procedure
        total number alive                                ▷ Collect summary of week wk:
        total number infected
    end for
end procedure
```

A.2 $\mathcal{R}_0$

We used the next generation matrix method described by Diekmann et al. to calculate $\mathcal{R}_0$ (eq. 8 - 10). β_1 is the transmission rate for the 0–14 age group; β_2 for the >15 group; γ is the common recovery rate.

$$F = \begin{pmatrix} \beta_1 & \beta_1 \\ \beta_2 & \beta_2 \end{pmatrix} \tag{8}$$

$$V = \begin{pmatrix} -\gamma & 0 \\ 0 & -\gamma \end{pmatrix} \tag{9}$$

$$\mathcal{R}_0 = \sqrt{eig(FV^{-}1)} = \sqrt{\frac{\beta_1 + \beta_2}{\gamma}} \tag{10}$$

A.3 Loss of immunity scenarios

We explored plausible scenarios of loss of immunity (Fig. A.1).

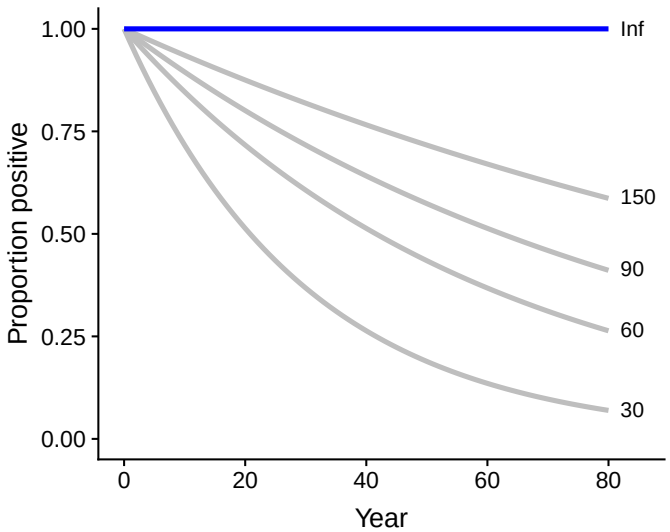

Figure A.1: Different scenarios of loss of immunity. No loss of immunity (blue) and scenarios explored (grey, exponential function with mean durations 30, 60, 90 and 150 years).

A.4 The number of infections introduced does influence the probability of an outbreak, but not the attack rate of successful outbreaks

The proportion of outbreaks (1% threshold) after introduction depends on the number of infections introduced; the attack rate of the successful outbreaks does not depend on the number of infections introduced (Fig. A.2).

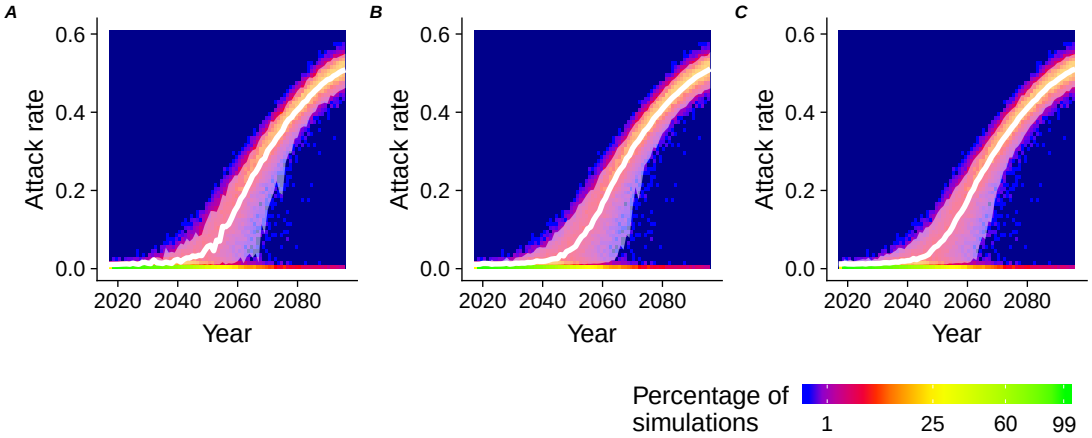

Figure A.2: Attack rate over time for the introduction of (A) n=1, (B) n=5, (C) n=10 infections.

A.5 Once per simulation introduction vs once per year introduction of infection

Using the ABM (model B) we explored the effect of yearly introduction of one infectious individual in the population (n=10,000). In the main text, we assumed a single introduction of n individuals per simulation. Here we introduce on a yearly basis the infectious individuals; previous outbreaks during the simulation affect the likelihood of a next outbreak and observed patterns are more stochastic. However, the pattern of the attack rate over time remains similar to the findings of the once/simulation introduction (Fig. A.3); the variation is larger due to a more stochasticity.

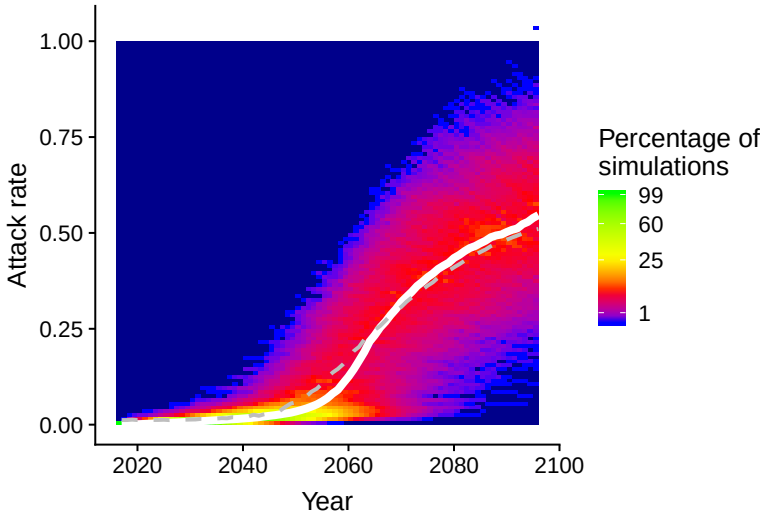

Figure A.3: Heat map of attack rate per time for simulations where every year one infectious individual is introduced in a population of 10,000. The median (white line) of this simulation is compared with the median of the simulation where once per simulation an infection is introduced (dashed grey line).

A.6 Comparison of SIR model with SEIR model and the Pandey model.

We compared the SIR model with a SEIR and model that explicitely models the vector; the Pandey 2013 model as implemented in Champagne et al. (2016) (Champagne et al., 2016). The model fit of the more complex models does not outperform the fit of the simplest (SIR) model (Table A.1), justifying the model choice.

Model	LOOIC (SE)	ΔLOOIC (SE)
SIR	95.2 (8.7)	Ref.
SEIR	93.9 (8.9)	-1.3 (1.6)
Pandey	99.5 (8.3)	4.3 (3.6)

Table A.1: Model comparison